Please cite this article in press as: Zhang et al., AgRP and POMC Neurons Are Hypophysiotropic and Coordinately Regulate Multiple Endocrine Axes in a Larval Teleost, Cell Metabolism (2012), doi:10.1016/j.cmet.2011.12.014

Cell Metabolism
Short Article

AgRP and POMC Neurons Are Hypophysiotropic and Coordinately Regulate Multiple Endocrine Axes in a Larval Teleost

Chao Zhang,[1,2] Paul M. Forlano,[3] and Roger D. Cone[1,*]
[1]Department of Molecular Physiology and Biophysics, Vanderbilt University School of Medicine, Nashville, TN 37232, USA
[2]Department of Cell and Developmental Biology, Oregon Health & Science University, Portland, OR 97239, USA
[3]Department of Biology and The Aquatic Research and Environmental Assessment Center, Brooklyn College and Graduate Center, The City University of New York, Brooklyn, NY 11210, USA
*Correspondence: roger.cone@vanderbilt.edu
DOI 10.1016/j.cmet.2011.12.014

SUMMARY

Plasticity in growth and reproductive behavior is found in many vertebrate species, but is common in male teleost fish. Typically, "bourgeois" males are considerably larger and defend breeding territories while "parasitic" variants are small and use opportunistic breeding strategies. The *P* locus mediates this phenotypic variation in *Xiphophorus* and encodes variant alleles of the melanocortin-4 receptor (MC4R). However, deletion of the MC4R has modest effects on somatic growth and reproduction in mammals, suggesting a fundamental difference in the neuroendocrine function of central melanocortin signaling in teleosts. Here we show in a teleost that the hypothalamic pro-opiomelanocortin and AgRP neurons are hypophysiotropic, projecting to the pituitary to coordinately regulate multiple pituitary hormones. Indeed, AgRP-mediated suppression of MC4R appears essential for early larval growth. This identifies the mechanism by which the central melanocortin system coordinately regulates growth and reproduction in teleosts and suggests it is an important anatomical substrate for evolutionary adaptation.

INTRODUCTION

Melanocortin-4 receptor (MC4R) signaling regulates energy homeostasis in vertebrate species from teleosts to humans (Farooqi et al., 2003; Huszar et al., 1997; Song and Cone, 2007; Vaisse et al., 1998; Yeo et al., 1998). The receptor is also known to regulate somatic growth from modest effects demonstrated in mammals (Farooqi et al., 2003; Huszar et al., 1997) to variant alleles in fish that can double the final length of animals (Lampert et al., 2010). Increased linear growth as a result of disruption of MC4R signaling has been reported in multiple mouse models, including agouti-related protein (AgRP) transgenic mice (Graham et al., 1997) and MC4R knockout mice (Huszar et al., 1997). Early studies in humans indicated an increased linear growth rate as early as a few months of age, when children with MC4R haploinsufficiency were compared with control obese children (Farooqi et al., 2003). More recently, MC4R haploinsufficiency in humans has also been demonstrated to be associated with a greater final attained height, relative to MC4R+/+ individuals matched for BMI. In human MC4R haploinsufficiency, there is no measurable increase in insulin-like growth factor I, and hyperinsulinemia has been suggested as a possible mechanism for the increased growth (Martinelli et al., 2011).

The central melanocortin system has also been demonstrated to be highly conserved in teleost fish. The receptors and ligands are expressed in a highly conserved pattern relative to mammals (Forlano and Cone, 2007; Song et al., 2003), and expression of the orexigenic melanocortin antagonist AgRP is dramatically upregulated during fasting in goldfish (Cerdá-Reverter and Peter, 2003) and zebrafish (Song et al., 2003), also as reported in mammals. Administration of MC4R agonists NDP-MSH or MTII inhibit food intake in goldfish (Cerdá-Reverter et al., 2003b) and rainbow trout (Schjolden et al., 2009), while i.c.v. injection of MC4R antagonists HS024 and SHU9119 stimulates food intake in fed goldfish (Cerdá-Reverter et al., 2003b) or rainbow trout (Schjolden et al., 2009). Experimental blockade of the MC4R by ectopic overexpression of AgRP increased body weight, body fat, and adult length in zebrafish (Song and Cone, 2007).

Recently, natural mutations affecting melanocortin signaling have also been characterized in fish. In the swordtail fish, *X. nigrensis* and *X. multilineatus*, small and large male morphs map to a single locus, *P* (Kallman and Borkoski, 1978), recently demonstrated to encode the MC4R (Lampert et al., 2010). Large male morphs in this species result from multiple copies of mutant forms of the receptor, at the Y chromosome-encoded *P* locus, which appear to function in a dominant-negative fashion, blocking activity of the wild-type receptor. Remarkably, these single-gene mutations also lead to altered onset of puberty and divergent reproductive strategies in the small- and large-size morphs. Because of the ease of genetic manipulation in the larval zebrafish, we sought to use this model system to better understand the role of MC4R signaling in somatic growth and reproduction in teleost fish.

RESULTS

agrp Is Required for Normal Somatic Growth of Larval Zebrafish

Since the endogenous antagonist of the MC4R, AgRP, is expressed as early as 1 day postfertilization (dpf) in the fish

Please cite this article in press as: Zhang et al., AgRP and POMC Neurons Are Hypophysiotropic and Coordinately Regulate Multiple Endocrine Axes in a Larval Teleost, Cell Metabolism (2012), doi:10.1016/j.cmet.2011.12.014

(Song et al., 2003), we designed *agrp* ATG targeting antisense morpholino oligonucleotides (MOs) to block translation of the *agrp* mRNA in larval growth, allowing for increased MC4R signaling. MOs are nondegradable synthetic nucleic acid analogs that can be designed to hybridize to complementary mRNA molecules to block translation or splicing (Summerton and Weller, 1997). Nontargeting standard control MOs and MOs targeting the other agouti genes (*asp* and *agrp2*) were also injected. Dose-responsive suppression of somatic growth was clearly seen in *agrp* morphants at 3–5 dpf (Figures 1A and 1B); a decrease in somite size, however, was documented, but no decrease in somite number (data not shown). An average body length of 4118 ± 23 μm (uninjected controls) or 4023 ± 46 μm (standard control MO injection) was reduced to 3045 ± 54 μm by injection of 2.5 ng *agrp* MO, for a 29% decrease in body length. MOs blocking *asp* (4137 ± 27 μm) or *agrp2* (4000 ± 23 μm) did not affect linear growth. We also designed two independent *agrp* MOs to block splicing of the *agrp* mRNA. These MOs were both demonstrated, using quantitative PCR (Q-PCR), to reduce full-length *agrp* mRNA levels by approximately 50% and to produce a statistically significant reduction in length at 5 dpf (9%–12% reduction; Figure S1).

Following MO injection and measurement at 5 dpf, fish were maintained as described (Experimental Procedures). At 14 dpf, the body length of ten randomly chosen fish from each condition was measured again with a micrometer. Growth normally plateaus temporarily around 5 dpf, and thus only slight further growth was seen in the uninjected or the control MO injected group (Figure 1C). However, at 14 dpf, *agrp* morphants receiving 2.5 ng of MO catch up in length, from 3045 ± 54 μm at 5 dpf to 3993 ± 33 μm at 14 dpf, although they were still somewhat shorter compared with uninjected control (4193 ± 55 μm) and 2.5 ng standard control morphants (4187 ± 58 μm). Thus, *agrp* MO injection does not cause a permanent developmental defect, since somatic growth catches up after inhibition of *agrp* expression by MO decays, around 3–7 days after injection.

Finally, we also demonstrated specificity using a rescue experiment. First, a construct was generated to produce *agrp* mRNA that was genetically altered to minimize the suppression of this mRNA by the *agrp* ATG blocking MO. Next, we coinjected 30 pg 5′ capped zebrafish *agrp* mRNA with 2.5 ng *agrp* MO oligo. Coinjection of 30 pg *agrp* RNA produced a significant rescue from the growth suppression resulting from 2.5 ng *agrp* MO (Figure 1D). These studies further support the hypothesis that normal larval growth specifically requires *agrp* expression.

agrp Regulates Somatic Growth via the *mc4r*

Zebrafish AgRP is an antagonist of 5 of the 6 zebrafish melanocortin receptors, with some specificity for the MC4R (Zhang et al., 2010). Several melanocortin receptor subtypes are expressed in the teleost CNS (Cerdá-Reverter et al., 2003a, 2003b; Klovins et al., 2004). To determine if the MC4R is the pharmacological target for the inhibition of somatic growth by MO blockade of *agrp*, we obtained three zebrafish *mc4r* mutant strains from the Sanger Institute Zebrafish Mutation Project. Wild-type zebrafish MC4R protein has 326 amino acids, while each *mc4r* mutant carries a nonsense mutation resulting in premature translation termination and expression of truncated proteins of 18, 30, or 185 amino acids; none of these truncated proteins could be expected to encode a functional GPCR protein (Figure 2A). As a control, we first examined the ability of *mc4r* loss to stimulate larval growth, since pharmacological blockade of the MC4R by *agrp* overexpression was shown to produce larger adult fish (Song and Cone, 2007). Heterozygous or homozygous loss of *mc4r* had no impact on length of fish at 5 dpf (Figure 2B) in sa0122 (sibling WT, 4002 ± 15 μM; heterozygous, 4008 ± 13 μM; homozygous, 4013 ± 16 μM), sa0148 (sibling WT, 3827 ± 20 μM; heterozygous, 3847 ± 16 μM; homozygous, 3822 ± 18 μM), or sa0149 (sibling WT, 3988 ± 21 μM; heterozygous, 3973 ± 16 μM; homozygous, 3997 ± 20 μM). Increased length resulting from homozygous loss of *mc4r* was detectable, however, as early as 42 dpf, and sustained in adult fish (Figures S2A–S2C).

To test the role of the *mc4r* in growth inhibition, 5 ng *agrp* MO oligo was injected into offspring of matings between sa0149 MC4R+/− fish. Significant growth retardation was seen in sibling WT (3103 ± 40 μM) compared with uninjected control fish (3978 ± 17 μM). *mc4r*−/− fish, however, appeared completely resistant to the growth-suppressing effects of *agrp* MO, retaining their body length (3960 ± 13 μM) in comparison with control group (3962 ± 16 μM) (Figures 2C and 2D). MOs designed to block *agrp* splicing (Figure S1) were also nonfunctional in the *mc4r*−/− background (data not shown). If the consequence of *agrp* blockade is enhanced stimulation of the MC4R by the endogenous ligand, α-MSH, then reduction of the *pomca* preprohormone gene encoding α-MSH should also reduce the consequences of *agrp* blockade. Indeed, coinjection of a *pomca* MO with *agrp* MO blunted the inhibition of somatic growth by *agrp* MO alone (Figure S2D). Together, the data support the hypothesis that *agrp* has a specific role in the regulation of somatic growth as an antagonist of α-MSH-mediated stimulation of MC4R signaling and that the MC4R must be inhibited by AgRP during the larval period for the normal rate of growth to occur. Interestingly, we observed that high levels of *agrp* mRNA are already observed in the embryo at 1 dpf, as previously reported (Song et al., 2003), but that melanocortin receptor expression appears to increase more gradually from 1 to 3 dpf (Figures S2E and S2F).

agrp Regulates Expression of Growth and Reproductive Hormones

Growth hormone is a key factor stimulating somatic growth in teleosts. While absence of *gh* alone does not reduce larval growth, *pit1* mutant zebrafish lacking growth hormone and prolactin exhibit severe dwarfism at 1 month of age (Nica et al., 2004). To identify the mechanism by which *mc4r* signaling regulates growth, expression of somatotropic and other pituitary hormones was examined. Whole-mount in situ hybridization at 4 dpf demonstrated a dramatic reduction of *gh* mRNA in pituitary (Figures 3A and 3B) following *agrp* MO injection. To determine if there was a general defect in pituitary gene expression, we examined expression of another pituitary preprohormone gene, pro-opiomelanocortin a (*pomca*, Figures 3C and 3D). *pomca* mRNA levels appeared unchanged. Next, we quantitated the relative expression at 4 dpf of *gh* and other genes involved in somatic growth and pituitary function by PCR. *gh* appeared downregulated 4-fold, while *ghrh* was upregulated 3.8-fold, and both somatostatin genes were decreased approximately

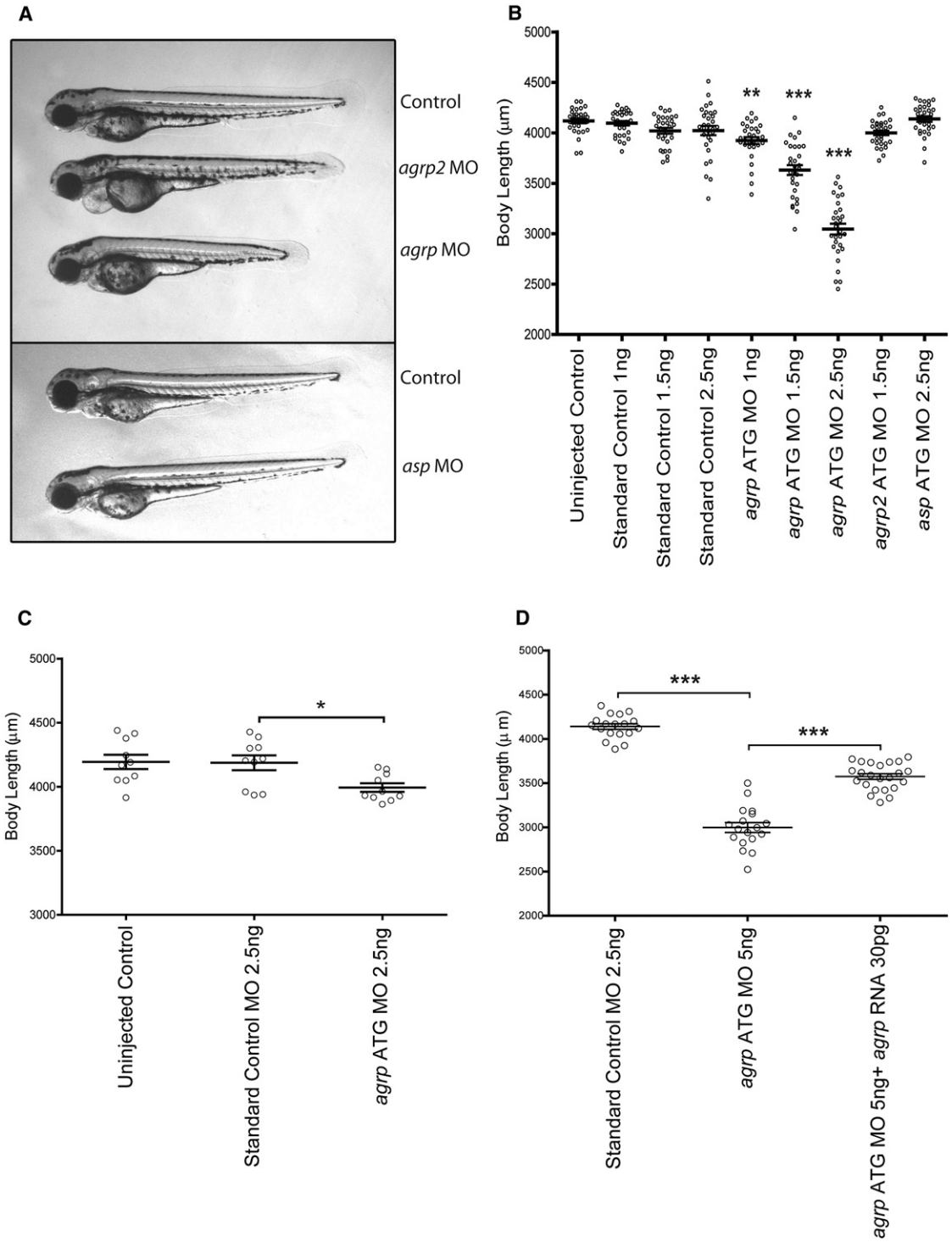

Figure 1. *agrp* Is Required for Normal Somatic Growth in Larval Zebrafish

(A–D) Representative fish at 3 dpf following injection at day 0 with morpholino oligonucleotides designed to inhibit expression of each of the zebrafish agouti proteins (A). Body lengths (jaw to tail fin) of injected fish were measured using a micrometer at 5 dpf, showing a dose-responsive inhibition of growth following morpholino blockade of *agrp* expression (B). Body lengths corresponding to fish injected at day 0 were measured at 14 dpf, showing partial restoration of length (C). Body lengths at 5 dpf following injection of zygotes with 5 ng morpholino oligonucleotide are indicated, plus 30 pg capped *agrp* RNA, where indicated, showing partial rescue of growth (D). Bars indicate mean ± SEM. n = 30 (B), 10 (C), and 18–23 (D). Statistical significance was tested by one-way ANOVA followed by Tukey's post test (*$p < 0.05$; **$p < 0.01$; ***$p < 0.001$). See also Figure S1.

Please cite this article in press as: Zhang et al., AgRP and POMC Neurons Are Hypophysiotropic and Coordinately Regulate Multiple Endocrine Axes in a Larval Teleost, Cell Metabolism (2012), doi:10.1016/j.cmet.2011.12.014

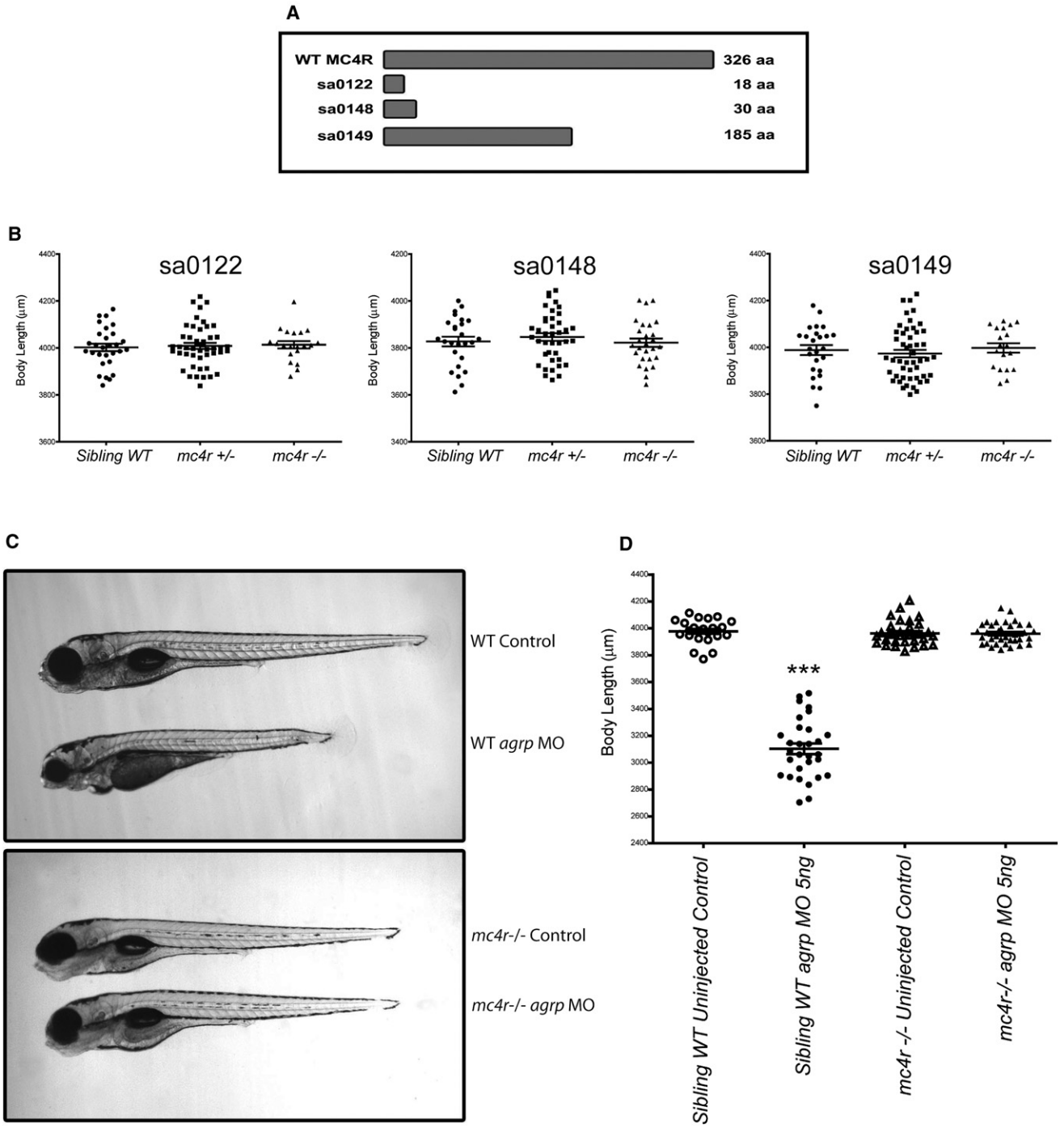

Figure 2. *mc4r* Is Required for Suppression of Somatic Growth by Morpholino Oligonucleotide Blockade of *agrp*

(A–D) Bar diagram showing the size of wild-type and mutant single *mc4r* coding alleles in three lines identified by TILLING (Sanger Institute) (A). The maximal potential protein coding segment of each receptor mutant is as follows: sa0122, 18 aa; sa0148, 30 aa; sa0149, 185 aa. *mc4r* mutations do not affect early larval growth (B). Offspring from heterozygote matings of sa0122, sa0148, and sa0149 were measured at 5 dpf, then genotyped by PCR. Numbers of fish analyzed in each group from left to right are 29, 47, 20 (sa0122); 26, 40, 27 (sa0148); and 25, 49, 19 (sa0149). Representative injected (5 ng agrp MO) or uninjected control sa0149 fish at 5 dpf with genotype and experimental treatment are indicated (C). Body lengths of fish treated as indicated (n = 24–36) were measured with a micrometer at 5 dpf, showing no effect of morpholino blockade of *agrp* on growth in the sa0149 *mc4r*−/− fish (D). Bars indicate mean ± SEM. Results were analyzed by one-way ANOVA followed by Tukey's post test (***$p < 0.001$). See also Figure S2.

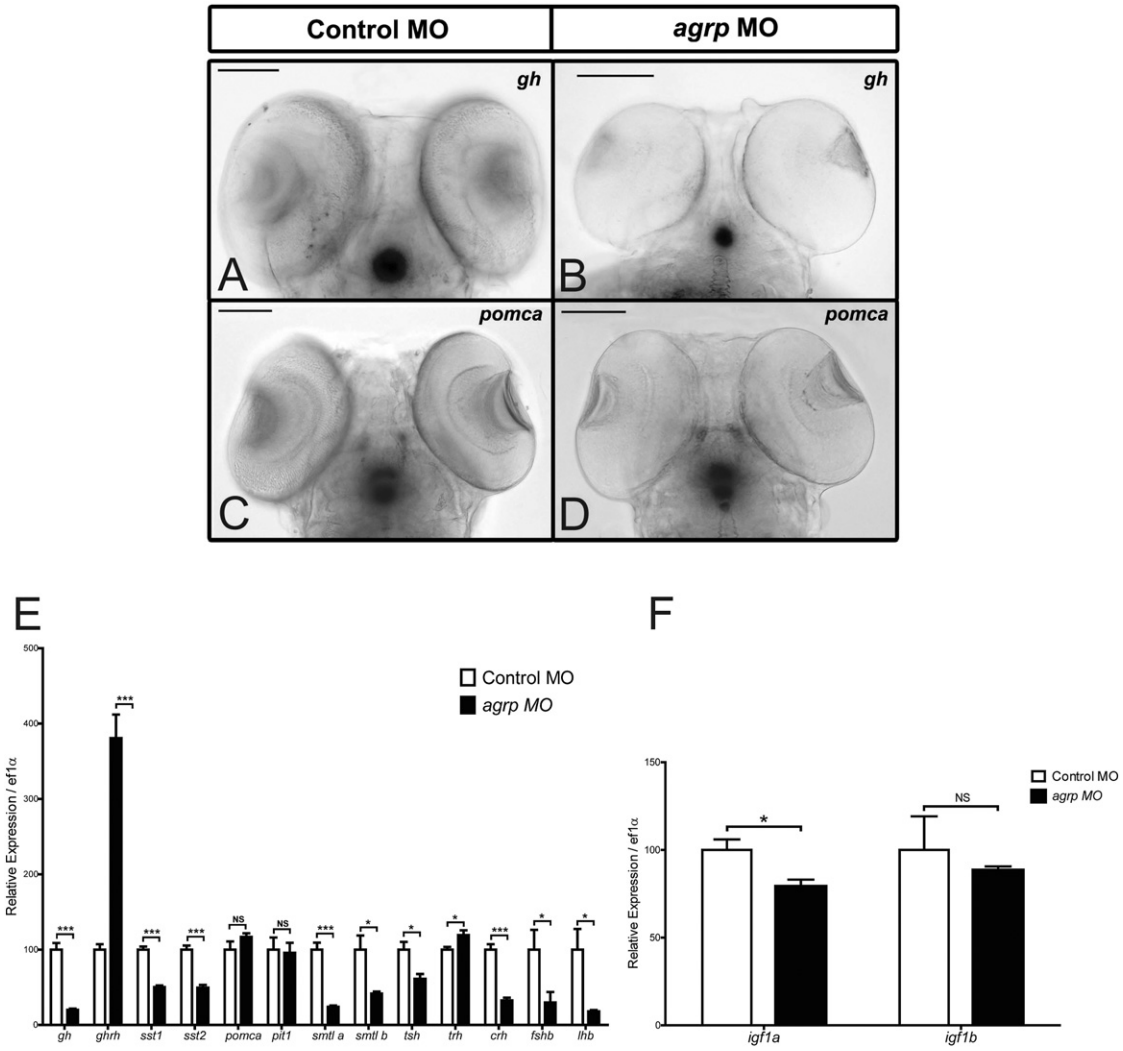

Figure 3. *agrp* Regulates Expression of Multiple Pituitary Hormones in Zebrafish

(A–F) Whole-mount in situ hybridization of *gh* (A and B) and *pomca* (C and D) in fish injected with 2.5 ng standard control (A and C) or *agrp* MO oligonucleotides (B and D). Scale bars: 100 μM. Relative expression levels of *gh* (growth hormone), *ghrh* (growth hormone-releasing hormone), *sst1* (somatostatin 1), *sst2* (somatostatin 2), *pomca* (pro-opiomelanocortin a), *pit1* (pituitary-specific positive transcription factor 1), *sml a* (somatolactin a), *sml b*, *tsh* (thyroid-stimulating hormone), *trh* (thyrotropin-releasing hormone), *crh* (corticotrophin-releasing hormone), *fshb* (follicle-stimulating hormone), *lhb* (luteinizing hormone), *igf1a* (insulin-like growth factor 1a), and *igf1b* were analyzed by Q-PCR in 30–40 4 dpf fish injected with 2.5 ng standard control or *agrp* MO oligonucleotides (E and F). mRNA expression was normalized to *ef1a* mRNA. Results were expressed as mean + SEM, and statistical analysis was done by unpaired t test (*$p < 0.05$; ***$p < 0.001$; NS, not significant). See also Figure S3.

50% (Figure 3E). The increase in hypothalamic *ghrh* and decrease in *sst1* and *sst2* gene expression argues that *agrp* blockade acts to block *gh* expression at the level of the pituitary, since the changes in *ghrh* and *sst1/sst2* would represent normal neuroendocrine compensation in response to decreased *gh* expression. Similarly, while pituitary *tsh* was suppressed, hypothalamic *trh* expression was elevated, also arguing for the pituitary as a primary site of action. Pituitary development appeared normal, as levels of expression of *pit1* and other pituitary genes such as *pomca* remained unchanged. As downstream mediators of the growth hormone pathway, insulin-like growth factors were also analyzed. One of the IGF genes, *igf1a*, was significantly reduced (Figure 3F). Interestingly, several other genes involved in neuroendocrine regulation were also altered specifically by *agrp* MO administration. For example, the reproductive hormones follicle-stimulating hormone b (*fshb*) and luteinizing hormone b (*lhb*) both appeared suppressed by *agrp* MO treatment (Figure 3E).

To confirm the role of the *mc4r* in regulation of the growth hormone axis by *agrp*, we also examined expression of *gh* and *pomca* by whole-mount in situ hybridization at 4 dpf in *mc4r*−/− fish treated with control or *agrp* MO. First, we characterized baseline levels of *pomca*, *pomcb*, *mc4r*, *agrp*, *gh*, and *ghrh* in WT and *mc4r*−/− fish by Q-PCR; no significant differences were seen. In contrast to WT fish, no change in *gh* expression was seen in *mc4r*−/− fish treated with *agrp* MO (Figure S3).

Please cite this article in press as: Zhang et al., AgRP and POMC Neurons Are Hypophysiotropic and Coordinately Regulate Multiple Endocrine Axes in a Larval Teleost, Cell Metabolism (2012), doi:10.1016/j.cmet.2011.12.014

AgRP-ir and POMC-ir Fibers Project to the Zebrafish Pituitary

The ability of *agrp* to regulate multiple pituitary hormones implied a unique neuroendocrine role for these neurons, and we thus sought to further characterize AgRP and POMC neuroanatomy in the larval zebrafish. Teleosts differ from mammals in hypothalamic-pituitary axis anatomy. The mammalian pituitary is functionally connected to the hypothalamus by the median eminence via a structure called the infundibular stem (pituitary stalk) (Low, 2008); in contrast, teleosts lack the hypothalamic-hypophysial-portal system, and hypophysiotropic neurons project directly into the anterior pituitary (Janz, 2000). The zebrafish pituitary sits juxtaposed to the lateral tuberal nucleus (the ventral periventricular hypothalamus, proposed homolog to the arcuate nucleus), where AgRP is primarily expressed (Forlano and Cone, 2007). To determine the anatomical basis for direct regulation of *gh*, *lhb*, *fshb*, and *tsh* by *agrp*, we sought to determine if AgRP-immunoreactive nerve fibers projected from the lateral tuberal nucleus to pituitary in the zebrafish. Double-labeled immunofluorescence was performed directly on brain sections from 5 dpf zebrafish, staining for AgRP and α-MSH. Confocal imaging of a horizontal section clearly shows zebrafish AgRP-ir fibers (green), originating in hypothalamic fiber bundles, projecting from hypothalamus to the posterior and rostral pars distalis (PPD, RPD), while fibers were largely absent in pars intermedia (PI, Figure 4). Putative pituitary melanotrope cell bodies staining positively for α-MSH (red) dominate the PI. While hypothalamic α-MSH-expressing POMC cell bodies, seen rostrally, are largely out of focus in this image, α-MSH-IR fibers are readily visible in the RPD and PPD. The AgRP-ir in the RPD appears to result from dense fiber bundles encircling cells, rather than staining of pituicytes. The inset is a magnification of a region of the PPD showing parallel AgRP-ir and α-MSH-ir neuronal fibers. These data indicate that hypothalamic AgRP and α-MSH fibers project to multiple subregions in the pituitary where many hormones are synthesized, including growth hormone, gonadotropins (FSH and LH), and prolactin (Kasper et al., 2006). Direct action of AgRP and/or POMC peptides such as α-MSH in pituitary would likely require expression of melanocortin receptors in this organ. Using RT-PCR with tissues from adult zebrafish, we identified zebrafish *mc4r* RNA expression in the pituitary gland (Figure S4).

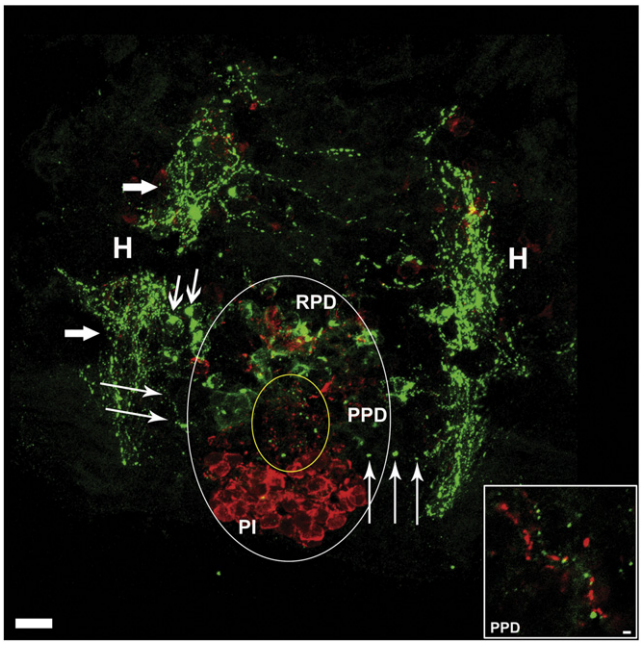

Figure 4. Hypothalamic AgRP- and α-MSH-Expressing Neurons Project to the Pituitary

Horizontal view of larval zebrafish brain at 5 dpf illustrating the pituitary and underlying hypothalamus. Large white oval approximates the extent of the pituitary, and small yellow oval indicates a zone within the proximal pars distalis containing dense α-MSH-immunoreactive (ir) fibers (red) and AgRP-ir fibers (green). Large arrows indicate hypothalamic AgRP-ir fiber bundles, medium arrows indicate hypothalamic AgRP-ir cell bodies, and thin arrows indicate AgRP-ir fibers projecting from hypothalamus into the pituitary. Inset is an enlargement from the PPD showing parallel AgRP-ir and α-MSH-ir neuronal fibers. PI, pars intermedia; PPD, proximal pars distalis; RPD, rostral pars distalis; H, hypothalamus. Scale bars: main image, 10 μm, inset = 1 μm.

DISCUSSION

The many ascending hypothalamic AgRP and POMC projections in the zebrafish exhibit conserved fiber pathways with their mammalian counterparts (Forlano and Cone, 2007). However, the data here represent a major neuroanatomical and functional departure for the teleost melanocortin system. In mammals, the melanocortin circuitry integrates information about energy stores with a subset of endocrine axes by serving as a leptin-responsive input to hypophysiotropic neurons in the hypothalamus, which in turn regulate pituitary hormone release (Cone, 2005; Tao, 2010). For example, the mammalian melanocortin circuits regulate the thyroid axis (Fekete et al., 2000a; Nillni et al., 2000). Using leptin-mediated regulation of the thyroid axis as an example, data show that TRH neurons in the paraventricular nucleus of the hypothalamus receive direct projections from arcuate POMC and AgRP neurons (Fekete et al., 2000b, 2000c; Harris et al., 2001; Perello et al., 2006; Toni et al., 1990). Leptin acts directly on these arcuate neurons (Bates et al., 2004; Elmquist et al., 1998; Hübschle et al., 2001; Perello et al., 2006) to control the release of α-MSH and AgRP, thus regulating the level of activity of the MC4R, and perhaps to some extent directly on the TRH neurons themselves (Ghamari-Langroudi et al., 2010), to regulate expression and release of TRH, and thus regulate activity of the thyroid axis. In contrast, mammalian melanocortin circuits have little impact on the reproductive axis (Irani et al., 2005) and have small effects on growth that do not appear to result from measurable increases, relative to normal individuals, in growth hormone or IGF expression (Martinelli et al., 2011). Some data suggest that the chronic blockade of the MC4R in the obese agouti mouse results in decreased hypothalamic somatostatin levels (Martin et al., 2006). Thus, the available data thus far indicate that in mammals, melanocortin circuits regulate endocrine function via control of the hypothalamic releasing hormone neurons.

In stark contrast to what is known in mammalian systems, data presented here demonstrate that the larval teleost POMC and AgRP neurons are hypophysiotropic, project to the pituitary, and directly and coordinately regulate expression of multiple endocrine axes. While the data indicate that *mc4r* mRNA is

Please cite this article in press as: Zhang et al., AgRP and POMC Neurons Are Hypophysiotropic and Coordinately Regulate Multiple Endocrine Axes in a Larval Teleost, Cell Metabolism (2012), doi:10.1016/j.cmet.2011.12.014

found in the pituitary, additional work will be needed to determine if functional MC4R is expressed in pituicytes such as the somatotropes and regulates hormones such as GH in direct response to AgRP and α-MSH released from hypophysiotropic AgRP and POMC neurons. During the first 5 dpf, zebrafish larvae do not feed, but rather acquire nutrients from the yolk sac. During this period, mutations in the *mc4r* do not measurably increase growth rate, which might be explained by the relatively high ratio of *agrp*/*pomca* expressed from 1 to 3 dpf producing chronic blockade of MC4R signaling (Figures S3E and S3F). In contrast, suppression of *agrp* expression reduces growth rate in a MC4R-dependent manner during this period. These data imply that MC4R suppression by AgRP is required for the maximal rate of growth during this period, allowing rapid maturation and thus perhaps reducing predation. In contrast, at some point after feeding behavior begins, during a period when growth and food intake can be regulated in response to environmental conditions, MC4R is no longer fully suppressed, and reduced MC4R activity, such as seen in mutant lines, can increase growth rate.

Taken together, the data provide a mechanistic basis for understanding natural variation in teleost growth and reproduction. Male size polymorphisms have been reported in many teleost species, including plainfin midshipman (Brantley and Bass, 1994), blenny (Oliveira et al., 2001), guppy (Tripathi et al., 2009), and swordtail platyfish (*Xiphophorus nigrensis* and *multilineatus*). The data presented here provide an anatomical and functional basis for the coregulation of growth and reproductive behavior seen in MC4R variants encoded by the *P* locus (Lampert et al., 2010). The central melanocortin system is thus a unique substrate for coordinate regulation of endocrine function and feeding and reproductive behavior. This, in turn, suggests that alterations in melanocortin signaling may play a role in the evolution of the diverse array of reproductive, growth, and feeding strategies observed in teleosts. Finally, in mammals, endocrine function is coordinated with energy state in large part via the action of the adipostatic hormone leptin (Ahima et al., 1996; Chehab et al., 1996) acting on independent hormone target sites in the hypothalamus that project to and regulate hypophysiotropic neurons. Leptin is poorly conserved in nonmammalian vertebrates and may not even exist in birds (Copeland et al., 2011); this, along with the unique ability of the central melanocortin circuits in teleosts to respond to energy state (Song et al., 2003) and coordinately regulate endocrine function, also implies significant differences in energy homeostasis between mammalian and nonmammalian vertebrates.

EXPERIMENTAL PROCEDURES

Experimental Animals

Wild-type Tab 14 or AB strain zebrafish were raised and bred at 26°C–28°C, with 14 hr light/10 hr dark cycle. Larval stage was determined according to Kimmel et al. (1995). Fish aged from 5 dpf to 10 dpf were fed twice a day with rotifers and baby powder, fish from 10 dpf to 15 dpf were fed with rotifer supplemented with uncapsulated brine shrimp, and fish from 15 dpf to 1 month or older were fed with uncapsulated brine shrimp. For adult fish, food was prepared by mixing 4 parts of tropical flakes (Aquatic Eco-Systems, Inc., Apopka, FL) and 1 part of brine shrimp (Brine Shrimp Direct, Ogden, UT) in system water. *mc4r*−/− mutant strains were obtained from the Sanger Institute Zebrafish Mutation Project and genotyped as described (Supplemental Information). All studies were approved by the animal care and use committee of Vanderbilt University.

RNA Extraction, cDNA Synthesis, and Real-Time Quantitative PCR

Embryos were homogenized in lysis buffer with a sonic dismembrator (model 100, Fisher Scientific, Pittsburgh, PA). Total RNA was extracted using an RNeasy Mini Kit (QIAGEN, Valencia, CA) according to the manufacturer's instructions. To remove genomic DNA, On-Column DNase Digestion was performed using an RNase-Free DNase Set (QIAGEN). One microgram of purified total RNA was reverse transcribed with iScript cDNA Synthesis Kit (Bio-Rad, Hercules, CA). Q-PCR primers were designed by Beacon Designer 7.0 (Premier Biosoft International, Palo Alto, CA) to minimize primer self-dimerization, and primer sequences are provided in the Supplemental Information. Q-PCRs were performed using 2 μl cDNA (20 ng) as template, 5 pmol of each of forward and reverse primers, and 2X Power SYBR PCR mix (Applied Biosystems, Carlsbad, CA) with nuclease free water (Promega, Madison, WI) to make the final volume to 20 ml in a 96-well plate (Bioexpress, Kaysville, UT). Q-PCRs were performed using an Mx3000PTM (Stratagene, Santa Clara, CA). The PCR cycle was performed according to manufacturer's instructions with initial denaturation at 95°C for 10 min, followed by 45 cycles of 95°C 20 s, 60°C 60 s. At the end of the cycles, melting curves of the products were verified for the specificity of PCR products. A standard curve with serial dilutions of cDNA sample was performed on each plate. All measurements were performed in duplicate, and prism 5.0 was used for the interpretation and analysis of data.

Whole-Mount In Situ Hybridization

To generate antisense digoxigenin (Dig)-labeled cRNA probes, pCr4-TOPO plasmids containing full-length *gh1* and *pomca* sequences (see Supplemental Information) were linearized by digestion with NotI and subjected to in vitro transcription with T3 RNA polymerase. For sense Dig-labeled cRNA probe, plasmids were linearized by digestion with SpeI and subjected to in vitro transcription with T7 RNA polymerase according to the manufacturer's protocol (Roche, Indianapolis, IN). Zebrafish embryos at different developmental stages were collected, manually dechorionated, and fixed in 4% paraformaldehyde in PBS at room temperature for 3–5 hr. Whole-mount in situ hybridization was performed as described previously (Westerfield, 2000). Briefly, fixed embryos were treated with −20°C methanol and rehydrated with a series of descending methanol concentrations (75%, 50%, and 25%) in PBS. They were then washed with PBS and treated with proteinase K (Fermentas, Glen Burnie, Maryland, MD) for 8 min at room temperature at a concentration of 10 μg/ml in PBS up to 24 hpf, 20 μg/ml from 24 hpf to 72 hpf and 50 μg/ml up to 15 dpf. Embryos were refixed with 4% paraformaldehyde in PBS at room temperature for 20 min, washed five times with PBS, prehybridized with hybridization buffer (50% formamide, 5× SSC, 50 μg/ml heparin [Sigma, St. Louis, MO], 500 μg/ml tRNA [Roche], 0.1% Tween-20, and 9.2 mM citric acid [pH.6.0]) at 65°C for 3 hr, then probed with either antisense or sense Dig-labeled probe at 65°C overnight at 500 ng/ml in hybridization buffer. Dig-labeled cRNA probes were detected with 1:2,000 diluted alkaline phosphatase conjugated anti-digoxigenin antibody (Roche) in 2% BMB (Roche) and 20% lamb serum (GIBCO BRL, Carlsbad, CA) in MAB (100 mM maleic acid, 150 mM NaCl, 0.1% Tween-20 [pH 7.5]) at 4°C overnight, followed by staining with NBT/BCIP solution (Roche) at room temperature for 2–5 hr. After PBS washing, methanol was applied to the stained embryos to remove the nonspecific stain and refixed in 4% paraformaldehyde in PBS. The embryos were mounted in 100% glycerol, and pictures were taken by AxioVision (Ver3.1) software with a Stemi SV11 Dissecting Microscope (Carl Zeiss).

Morpholino Oligonucleotide Injection, RNA Rescue Experiment, and Body Length Measurement

MOs, prepared as described (Supplemental Information), were dissolved in nuclease-free water and stored in −20°C as 1 mM stock. Serial dilutions were made using nuclease-free water to 0.1, 0.2, 0.3, and 0.4 mM working solution with 20% Phenol Red (Sigma; 0.5% in DPBS, sterile filtered, endotoxin tested). Before the injection, MOs were denatured at 65°C for 5 min and quickly spun to avoid the formation of aggregates. Three to five microliters was loaded in a microinjection machine, and embryos at one or two cell stages were injected with1–2 nl of a solution containing antisense targeting morpholino or standard control oligo. Each MO oligo injection was repeated at least three times, and doses were adjusted to optimize the phenotype-to-toxicity ratio. Following morpholino injections, embryos were raised in egg water,

changed daily, under standard light/dark cycle up to 6 dpf. Dead embryos were excluded at 1 dpf. Embryos were assayed for whole-mount in situ hybridization and quantitative RT-PCR at 4 dpf. Linear body length (forehead to tail fin) was determined using a micrometer at 5 dpf, 14 dpf, and 42 dpf. Embryos were mounted in 2.5% methyl cellulose, and images were taken by AxionVision (Ver3.1) software with a Lumar V12 Stereo Microscope (Carl Zeiss).

Full-length *agrp* including 5′ UTR sequence for mRNA rescue was cloned into PCS2+ vector, which contains a 5′ SP6 promoter and 3′ SV40 polyA tail. To make 5′ capped zebrafish *agrp* RNA, plasmids were linearized by digestion with NotI and subjected to in vitro transcription with SP6 RNA polymerase in the presence of 0.5 mM Ribo m7G Cap Analog (Promega). RNA was purified by mini Quick Spin Column (Roche) according to the manufacturer's instructions. *agrp* ATG antisense MO was injected at 0.3 mM with or without 30 ng/μl capped *agrp* RNA. Embryos were raised at standard dark/light cycle and body length was measured at 5 dpf.

Immunocytochemistry

Zebrafish larvae were anesthetized in MS222 (tricaine methanesulfonate, Sigma) on ice and fixed whole with teleost Ringer's solution followed by 4% paraformaldehyde in 0.1 M phosphate buffer (PB, pH 7.2) for 1 hr at RT. After fixation, larvae were washed in PB and cryoprotected in 30% sucrose in PB overnight at 4°C. They then were embedded in Tissue-TeK OCT medium (Sakura Finetek, Torrance, CA) in Tissue-Tek intermediate cryomolds, stored at −80°C until being sectioned on a cryostat in the transverse, sagittal, or horizontal plane at 16 μm, and collected onto Superfrost Plus slides (Fisher Scientific, Fair Lawn, NJ). The immunocytochemical labeling protocol followed Forlano and Cone (2007), and slides were coverslipped with SlowFade Gold with DAPI (Molecular Probes, Carlsbad, CA) nuclear counterstain to provide cytoarchitectonic detail. Micrographs were taken on a Zeiss LSM 710 META Inverted Confocal Microscope.

SUPPLEMENTAL INFORMATION

Supplemental Information includes Supplemental Experimental Procedures and four figures and can be found with this article online at doi:10.1016/j.cmet.2011.12.014.

ACKNOWLEDGMENTS

Supported by NIH grant RO1DK075721 (R.D.C.). The authors would like to thank Drs. Sam Wells and Bob Matthews for help with confocal microscopy.

Received: September 7, 2011
Revised: November 23, 2011
Accepted: December 23, 2011
Published online: January 12, 2012

REFERENCES

Ahima, R.S., Prabakaran, D., Mantzoros, C., Qu, D., Lowell, B., Maratos-Flier, E., and Flier, J.S. (1996). Role of leptin in the neuroendocrine response to fasting. Nature *382*, 250–252.

Bates, S.H., Dundon, T.A., Seifert, M., Carlson, M., Maratos-Flier, E., and Myers, M.G., Jr. (2004). LRb-STAT3 signaling is required for the neuroendocrine regulation of energy expenditure by leptin. Diabetes *53*, 3067–3073.

Brantley, R.K., and Bass, A.H. (1994). Alternative Male Spawning Tactics and Acoustic Signals in the Plainfin Midshipman Fish Porichthys notatus Girard (Teleostei, Batrachoididae). Ethology *96*, 213–232.

Cerdá-Reverter, J.M., and Peter, R.E. (2003). Endogenous melanocortin antagonist in fish: structure, brain mapping, and regulation by fasting of the goldfish agouti-related protein gene. Endocrinology *144*, 4552–4561.

Cerdá-Reverter, J.M., Ling, M.K., Schiöth, H.B., and Peter, R.E. (2003a). Molecular cloning, characterization and brain mapping of the melanocortin 5 receptor in the goldfish. J. Neurochem. *87*, 1354–1367.

Cerdá-Reverter, J.M., Ringholm, A., Schiöth, H.B., and Peter, R.E. (2003b). Molecular cloning, pharmacological characterization, and brain mapping of the melanocortin 4 receptor in the goldfish: involvement in the control of food intake. Endocrinology *144*, 2336–2349.

Chehab, F.F., Lim, M.E., and Lu, R. (1996). Correction of the sterility defect in homozygous obese female mice by treatment with the human recombinant leptin. Nat. Genet. *12*, 318–320.

Cone, R.D. (2005). Anatomy and regulation of the central melanocortin system. Nat. Neurosci. *8*, 571–578.

Copeland, D.L., Duff, R.J., Liu, Q., Prokop, J., and Londraville, R.L. (2011). Leptin in teleost fishes: an argument for comparative study. Front Physiol *2*, 26.

Elmquist, J.K., Bjørbaek, C., Ahima, R.S., Flier, J.S., and Saper, C.B. (1998). Distributions of leptin receptor mRNA isoforms in the rat brain. J. Comp. Neurol. *395*, 535–547.

Farooqi, I.S., Keogh, J.M., Yeo, G.S., Lank, E.J., Cheetham, T., and O'Rahilly, S. (2003). Clinical spectrum of obesity and mutations in the melanocortin 4 receptor gene. N. Engl. J. Med. *348*, 1085–1095.

Fekete, C., Légrádi, G., Mihály, E., Huang, Q.-H., Tatro, J.B., Rand, W.M., Emerson, C.H., and Lechan, R.M. (2000a). α-Melanocyte-stimulating hormone is contained in nerve terminals innervating thyrotropin-releasing hormone-synthesizing neurons in the hypothalamic paraventricular nucleus and prevents fasting-induced suppression of prothyrotropin-releasing hormone gene expression. J. Neurosci. *20*, 1550–1558.

Fekete, C., Légrádi, G., Mihály, E., Huang, Q.H., Tatro, J.B., Rand, W.M., Emerson, C.H., and Lechan, R.M. (2000b). alpha-Melanocyte-stimulating hormone is contained in nerve terminals innervating thyrotropin-releasing hormone-synthesizing neurons in the hypothalamic paraventricular nucleus and prevents fasting-induced suppression of prothyrotropin-releasing hormone gene expression. J. Neurosci. *20*, 1550–1558.

Fekete, C., Mihály, E., Luo, L.-G., Kelly, J., Clausen, J.T., Mao, Q., Rand, W.M., Moss, L.G., Kuhar, M., Emerson, C.H., et al. (2000c). Association of cocaine- and amphetamine-regulated transcript-immunoreactive elements with thyrotropin-releasing hormone-synthesizing neurons in the hypothalamic paraventricular nucleus and its role in the regulation of the hypothalamic-pituitary-thyroid axis during fasting. J. Neurosci. *20*, 9224–9234.

Forlano, P.M., and Cone, R.D. (2007). Conserved neurochemical pathways involved in hypothalamic control of energy homeostasis. J. Comp. Neurol. *505*, 235–248.

Ghamari-Langroudi, M., Vella, K.R., Srisai, D., Sugrue, M.L., Hollenberg, A.N., and Cone, R.D. (2010). Regulation of thyrotropin-releasing hormone-expressing neurons in paraventricular nucleus of the hypothalamus by signals of adiposity. Mol. Endocrinol. *24*, 2366–2381.

Graham, M., Shutter, J.R., Sarmiento, U., Sarosi, I., and Stark, K.L. (1997). Overexpression of Agrt leads to obesity in transgenic mice. Nat. Genet. *17*, 273–274.

Harris, M., Aschkenasi, C., Elias, C.F., Chandrankunnel, A., Nillni, E.A., Bjøorbaek, C., Elmquist, J.K., Flier, J.S., and Hollenberg, A.N. (2001). Transcriptional regulation of the thyrotropin-releasing hormone gene by leptin and melanocortin signaling. J. Clin. Invest. *107*, 111–120.

Hübschle, T., Thom, E., Watson, A., Roth, J., Klaus, S., and Meyerhof, W. (2001). Leptin-induced nuclear translocation of STAT3 immunoreactivity in hypothalamic nuclei involved in body weight regulation. J. Neurosci. *21*, 2413–2424.

Huszar, D., Lynch, C.A., Fairchild-Huntress, V., Dunmore, J.H., Fang, Q., Berkemeier, L.R., Gu, W., Kesterson, R.A., Boston, B.A., Cone, R.D., et al. (1997). Targeted disruption of the melanocortin-4 receptor results in obesity in mice. Cell *88*, 131–141.

Irani, B.G., Xiang, Z., Moore, M.C., Mandel, R.J., and Haskell-Luevano, C. (2005). Voluntary exercise delays monogenetic obesity and overcomes reproductive dysfunction of the melanocortin-4 receptor knockout mouse. Biochem. Biophys. Res. Commun. *326*, 638–644.

Janz, D.M. (2000). Endocrine System. In The Laboratory Fish, G.K. Ostrander, ed. (Boston: Academic Press), pp. 190–191.

Kallman, K.D., and Borkoski, V. (1978). A Sex-Linked Gene Controlling the Onset of Sexual Maturity in Female and Male Platyfish (XIPHOPHORUS

MACULATUS), Fecundity in Females and Adult Size in Males. Genetics *89*, 79–119.

Kasper, R.S., Shved, N., Takahashi, A., Reinecke, M., and Eppler, E. (2006). A systematic immunohistochemical survey of the distribution patterns of GH, prolactin, somatolactin, beta-TSH, beta-FSH, beta-LH, ACTH, and alpha-MSH in the adenohypophysis of Oreochromis niloticus, the Nile tilapia. Cell Tissue Res. *325*, 303–313.

Kimmel, C.B., Ballard, W.W., Kimmel, S.R., Ullmann, B., and Schilling, T.F. (1995). Stages of embryonic development of the zebrafish. Dev. Dyn. *203*, 253–310.

Klovins, J., Haitina, T., Fridmanis, D., Kilianova, Z., Kapa, I., Fredriksson, R., Gallo-Payet, N., and Schiöth, H.B. (2004). The melanocortin system in Fugu: determination of POMC/AGRP/MCR gene repertoire and synteny, as well as pharmacology and anatomical distribution of the MCRs. Mol. Biol. Evol. *21*, 563–579.

Lampert, K.P., Schmidt, C., Fischer, P., Volff, J.N., Hoffmann, C., Muck, J., Lohse, M.J., Ryan, M.J., and Schartl, M. (2010). Determination of onset of sexual maturation and mating behavior by melanocortin receptor 4 polymorphisms. Curr. Biol. *20*, 1729–1734.

Low, M.J. (2008). Neuroendocrinology. In Williams Textbook of Endocrinology, H.M. Kronenberg, S. Melmed, K.S. Polonsky, and P.R. Larsen, eds. (Philadelphia: Saunders Elsevier), pp. 85–154.

Martin, N.M., Houston, P.A., Patterson, M., Sajedi, A., Carmignac, D.F., Ghatei, M.A., Bloom, S.R., and Small, C.J. (2006). Abnormalities of the somatotrophic axis in the obese agouti mouse. Int J Obes (Lond) *30*, 430–438.

Martinelli, C.E., Keogh, J.M., Greenfield, J.R., Henning, E., van der Klaauw, A.A., Blackwood, A., O'Rahilly, S., Roelfsema, F., Camacho-Hübner, C., Pijl, H., and Farooqi, I.S. (2011). Obesity due to melanocortin 4 receptor (MC4R) deficiency is associated with increased linear growth and final height, fasting hyperinsulinemia, and incompletely suppressed growth hormone secretion. J. Clin. Endocrinol. Metab. *96*, E181–E188.

Nica, G., Herzog, W., Sonntag, C., and Hammerschmidt, M. (2004). Zebrafish pit1 mutants lack three pituitary cell types and develop severe dwarfism. Mol. Endocrinol. *18*, 1196–1209.

Nillni, E.A., Vaslet, C., Harris, M., Hollenberg, A., Bjørbak, C., and Flier, J.S. (2000). Leptin regulates prothyrotropin-releasing hormone biosynthesis. Evidence for direct and indirect pathways. J. Biol. Chem. *275*, 36124–36133.

Oliveira, R.F., Carneiro, L.A., Canario, A.V., and Grober, M.S. (2001). Effects of androgens on social behavior and morphology of alternative reproductive males of the Azorean rock-pool blenny. Horm. Behav. *39*, 157–166.

Perello, M., Stuart, R.C., and Nillni, E.A. (2006). The role of intracerebroventricular administration of leptin in the stimulation of prothyrotropin releasing hormone neurons in the hypothalamic paraventricular nucleus. Endocrinology *147*, 3296–3306.

Schjolden, J., Schiöth, H.B., Larhammar, D., Winberg, S., and Larson, E.T. (2009). Melanocortin peptides affect the motivation to feed in rainbow trout (Oncorhynchus mykiss). Gen. Comp. Endocrinol. *160*, 134–138.

Song, Y., and Cone, R.D. (2007). Creation of a genetic model of obesity in a teleost. FASEB J. *21*, 2042–2049.

Song, Y., Golling, G., Thacker, T.L., and Cone, R.D. (2003). Agouti-related protein (AGRP) is conserved and regulated by metabolic state in the zebrafish, Danio rerio. Endocrine *22*, 257–265.

Summerton, J., and Weller, D. (1997). Morpholino antisense oligomers: design, preparation, and properties. Antisense Nucleic Acid Drug Dev. *7*, 187–195.

Tao, Y.X. (2010). The melanocortin-4 receptor: physiology, pharmacology, and pathophysiology. Endocr. Rev. *31*, 506–543.

Toni, R., Jackson, I.M., and Lechan, R.M. (1990). Neuropeptide-Y-immunoreactive innervation of thyrotropin-releasing hormone-synthesizing neurons in the rat hypothalamic paraventricular nucleus. Endocrinology *126*, 2444–2453.

Tripathi, N., Hoffmann, M., Willing, E.M., Lanz, C., Weigel, D., and Dreyer, C. (2009). Genetic linkage map of the guppy, Poecilia reticulata, and quantitative trait loci analysis of male size and colour variation. Proc. Biol. Sci. *276*, 2195–2208.

Vaisse, C., Clement, K., Guy-Grand, B., and Froguel, P. (1998). A frameshift mutation in human MC4R is associated with a dominant form of obesity. Nat. Genet. *20*, 113–114.

Westerfield, M. (2000). The Zebrafish Book. A guide for the laboratory use of zebrafish (Eugene, OR: University of Oregon Press).

Yeo, G.S.H., Farooqi, I.S., Aminian, S., Halsall, D.J., Stanhope, R.G., and O'Rahilly, S. (1998). A frameshift mutation in MC4R associated with dominantly inherited human obesity. Nat. Genet. *20*, 111–112.

Zhang, C., Song, Y., Thompson, D.A., Madonna, M.A., Millhauser, G.L., Toro, S., Varga, Z., Westerfield, M., Gamse, J., Chen, W., and Cone, R.D. (2010). Pineal-specific agouti protein regulates teleost background adaptation. Proc. Natl. Acad. Sci. USA *107*, 20164–20171.

Cell Metabolism, Volume *15*
Supplemental Information

AgRP and POMC Neurons Are Hypophysiotropic and Coordinately Regulate Multiple Endocrine Axes in a Larval Teleost

Chao Zhang, Paul M. Forlano, and Roger D. Cone

SUPPLEMENTAL EXPERIMENTAL PROCEDURES

Morpholino oligonucleotides

Antisense morpholino oligonucleotide (MO) against the ATG translation initiation site of *agrp*, *agrp2*, *asp*, *pomca* and standard control MO, and MO against splice sites of agrp were designed and synthesized by GeneTools, LLC (Philomath, OR USA): *agrp* ATG MO: 5' ACTGTGTTCAGCATCATAATCACTC 3', *agrp2* ATG MO: 5'TTTCAGCACCGCCGTCGTCATTTTC3', *agrp* E1I1 MO: 5'ACTTACCTGTGTCAGATGTCAGAAT 3', *agrp* I1E2 MO: 5'GCAGTGAGTCTATGATGTACAAAAC 3', *asp* ATG MO: 5'AGCACAGCCACAATGACGGACTCAT3' *pomca* ATG MO: 5' ACAACATCCTCACTCCCCTCACCAT 3'

Primers used for Q-PCR and PCR

gh1 (growth hormone 1), forward primer 5' GCAGTTGGTGGTGGTTAG 3', reverse primer 5' GCGTTCCTCAGGCATAAG 3'. *ghrh* (growth hormone releasing hormone), forward primer 5' GTGCTATGCTGCTTGTTACTATC 3', reverse primer 5' ATACTTGACTGACGCTTTACATTG 3'. *pomca* (proopiomelanocortin a), forward primer 5' TCTTGGCTCTGGCTGTTC 3', reverse primer 5' TCGGAGGGAGGCTGTAG 3'. *sst1* (somatostatin 1), forward primer 5' CCAAACTCCGCCAACTTC 3', reverse primer 5' CTCCAGACGCACATCATC 3'. *sst2* (somatostatin 2), forward primer 5' AGCAACTCTTCTCTGTCTGG 3', reverse primer 5' TCTCTGGTATCTCTTCATCCG 3'.

igf1a (insulin-like growth factor 1a), forward primer 5’ GGTGCTGTGCGTCCTC 3’, reverse primer 5’ GTCCATATCCTGTCGGTTTG 3’. *igf1b* (insulin-like growth factor 1b), forward primer 5’ GGTGGTCCTCGCTCTC 3’, reverse primer 5’ TCTGCTAACTTCTGGTATCG 3’. *pit1* (pituitary specific transcription factor 1), forward primer 5’ GGTCCAGTCGTCCAAG 3’, reverse primer 5’ TTCCTGTGCTGCCATC 3’. *somatolactin a*, forward primer 5’ TGGTTCAGTCGTGGATGG 3’, reverse primer 5’ AAGATGGTGGAGGATGCC 3’. *somatolactin b*, forward primer 5’ TCTCGGAGGAAGCCAAGTTG 3’, reverse primer 5’ AGCCATCGGTCGGAAATCTG 3’. *crh* (corticotropin releasing hormone), forward primer 5’ CTCTGCTCGTTGCCTTTC 3’, reverse primer 5’ GACTGCCGCTCTCCATC 3’. *trh* (thyrotropin-releasing hormone), forward primer 5’ CGCTCCATCCTCACAC 3’, reverse primer 5’ CGCTCCATCTTCACCTC 3’. *tsh* (thyroid-stimulating hormone), forward primer 5’ ACTGTGTGGCTGTCAAC 3’, reverse primer 5’ CTGGGTAGGTGAAGTGAG 3’. *agrp*, forward primer F1 5’GTGAATGTTGTGGTGATG3’
agrp, reverse primer R2 5’TTCTTCTGCTGAGTTTATTTC3’,
agrp, reverse primer R3 5’ACTGTTGATGAGGGATAC3’. All gene expression was normalized to house-keeping gene, ef1α (Elongation Factor 1 alpha), with forward primer 5’ CTGGAGGCCAGCTCAAACAT 3’, reverse primer 5’ ATCAAGAAGAGTAGTACCGCTAGCATTAC 3’.

Primers used for cloning

Full length *gh1* and *pomca* sequences were cloned into pCR4-TOPO vector (Invitrogen, Carlsbad, CA, USA) using *t*he following primers: zGH1 full F (forward): 5’ CTTGGACAAAATGGCTAGAGCATTG 3’, zGH1 full R (reverse): 5’ AGCAATACATTAGCGCCCTCTACAG 3’. zPOMCa full F (forward): 5’ CGGGATCCCTTTGGTTACTGACTTCTTTC 3’, zPOMCa full R (reverse): 5’ CGGGATCCGACCCCCTATAACAACCTCTCC 3’.

Full length *agrp* was cloned using the following primers: zAgRP RNA BamHI full F (forward): 5’ AACGGATCCAGCCTGGGACGTGAGCACTACAGTCTG 3’, zAgRP RNA XbaI full R (reverse): 5’ AACTCTAGATCTCTATGCATATTCGTTTTTGCAGG 3’.

Genotyping *mc4r* mutants

Genomic DNA was prepared from embryos or tail fin clips as follows. Embryo or fin tissue was placed into 100 µl 50mM NaOH and heated to 95 °C for 20 minutes. Tubes were cooled to room temperature, then 10µl 1M Tris-HCl buffer (PH 8.0) was added. Tubes were centrifuged at14 K rpm for 2 minutes, and supernatant was removed and stored at –20 °C. Primers used for RFLP (Restriction Fragment Length Polymorphism) amplification: for sa0122 and sa0148, zMC4R genotype F: 5’ TGATCTACATGGTGGATGATG 3’; zMC4R genotype R: 5’ TGAGGCAGATGAGAACAGTG 3’. For sa0149, zMC4R genotype F2: 5’ GACCGCTACATCACAATCTTC 3’; zMC4R genotype R2: 5’ TCCAGTTGCTAAGTGCTGTC 3’. DNA was amplified with primers and 2µl supernatant in a 15 µl reaction using 2X GoTaq Green Master Mix (Promega, Madison, MI, USA) with initial denaturation at 94 °C for 3 min, followed by 40 cycles of 94 °C for 20 s, 58 °C for 20 s, 72 °C for 60 s with final extension at 72 °C for 5 min. Prior to agarose gel electrophoresis, DNA was digested with NEB (New England Biolabs, Ipswich, MA, USA) restriction enzymes in PCR mix according to manufacturer’s manual. For sa0122, StyI was used for digestion with expected DNA bands 146bp and 534bp for wild type; 146bp, 534bp and 680bp for *mc4r*+/-; 680bp for *mc4r*-/-. For sa0148, DdeI was used for digestion with expected DNA bands 680bp for wild type; 185bp, 495bp and 680bp for *mc4r*+/-; 185bp and 495bp for *mc4r*-/-. For sa0149, MseI was used for digestion with expected DNA bands 588bp for wild type; 127bp, 461bp and 588bp for *mc4r*+/-; 127bp and 461bp for *mc4r*-/-.

SUPPLEMENTAL FIGURES

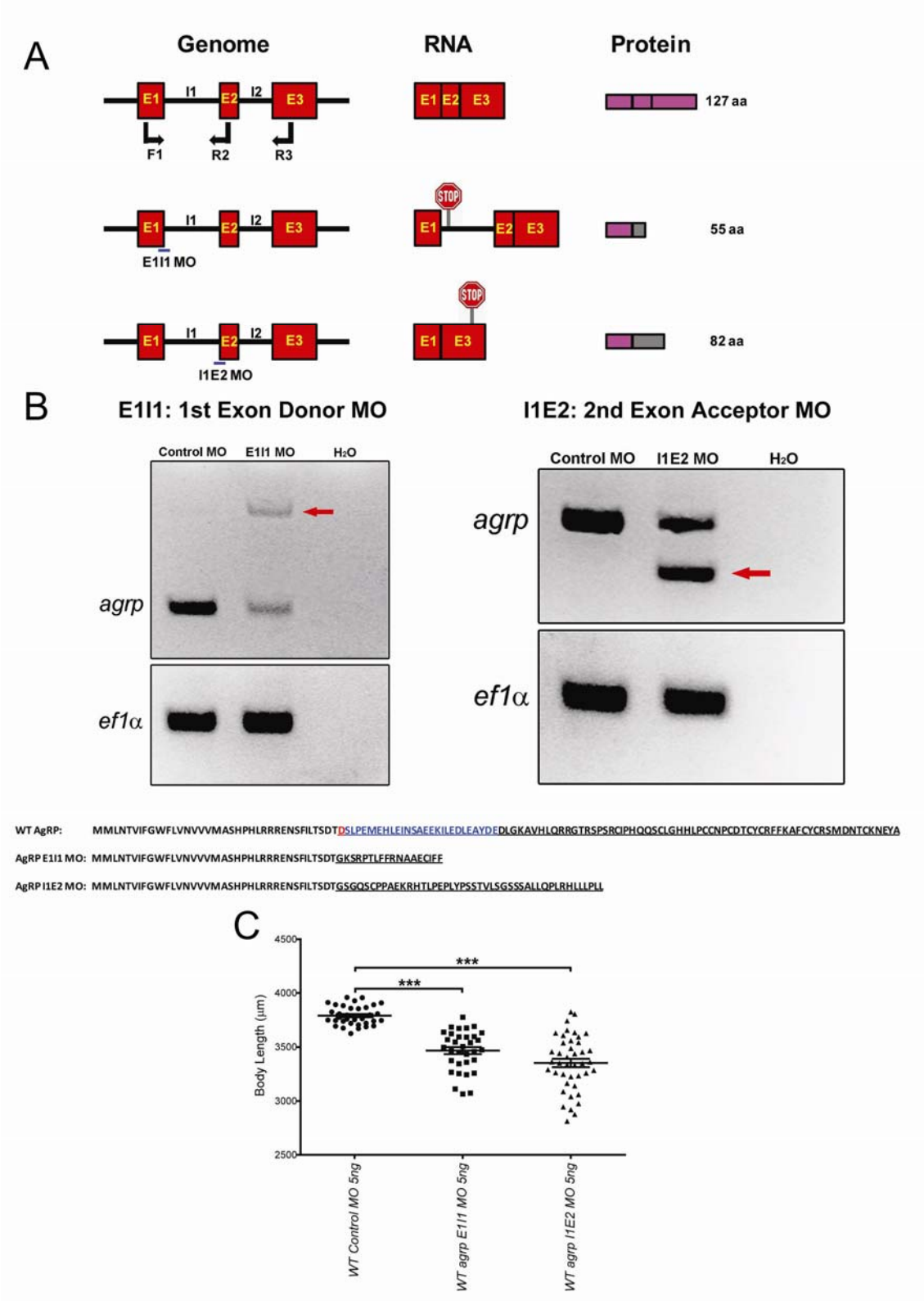

Figure S1. Morpholino Oligonucleotides Blocking *agrp* Splicing Reduce Normal Somatic Growth in Larval Zebrafish.

(A) Bar diagram showing the targets and predicted consequences of two morpholino oligonucleotides designed to block splicing of the *agrp* mRNA. (B) Efficiency of each antisense MO was confirmed by RT-PCR at 2dpf. Red arrows show predicted longer form of *agrp* RNA with disruption of the first splice donor (E1I1, left panel) and shorter form of *agrp* RNA resulting from blockade of first splice acceptor (I1E2, right panel), as seen on agarose gel from *agrp* E1I1 exon donor morphant and *agrp* I1E2 exon acceptor morphant, respectively. Predicted protein sequences of WT and morphant AgRP proteins are indicated. (C) Body lengths of fish injected with standard control MO, E1I1 MO and I1E2 MO were measured with a micrometer at 5dpf. Bars indicates mean±s.e.m. Results were analyzed by one way ANOVA followed by Tukey post test. (n=36, 33 and 42. ***, $p<0.001$).

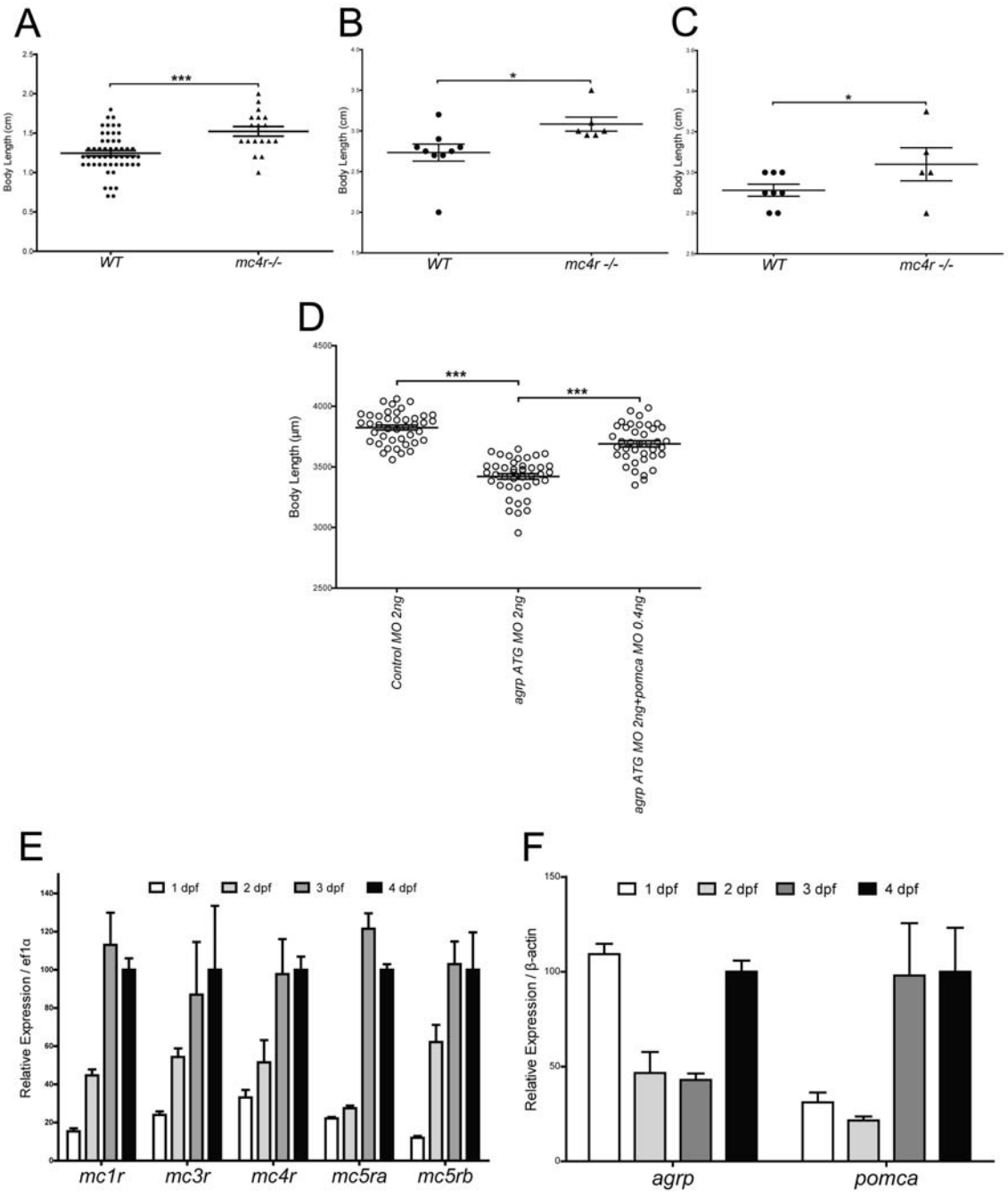

Figure S2. Role of MC4R, AgRP and POMC in Zebrafish Growth

(A-C) *mc4r-/-* fish exhibit increased growth by 42 dpf. Fish from a sa0149 mc4r +/- intercrossing were allowed to grow to adulthood. Body lengths (jaw to trunk terminus, tail fin excluded) of juveniles were measured at 42 days post fertilization (A). Female (B) and male (C) adult zebrafish were also measured at 8 months. Bars indicate mean±s.e.m. Results were analyzed by one way ANOVA followed by Tukey post test. (N=5-53, *P<0.05;***P<0.001). (D) Partial

rescue of *agrp* MO inhibition of somatic growth by co-injection of *pomca* MO. Body lengths at 5 dpf following injection of wild type zygotes with 2 ng MO indicated, plus 0.4ng *pomca* ATG antisense MO showing partial rescue of growth. Bars indicates mean±s.e.m. n= 42, 42, 39. Statistical significance tested by one way ANOVA followed by Tukey post test. (***, $p<0.001$). (E-F) Developmental expression of melanocortin receptor and ligand genes. Relative expression levels of (E) *mc1r, mc3r, mc4r, mc5ra, and mc5rb,* and (F) *agrp* and *pomca* were analyzed by Q-PCR. ~200 WT zebrafish zygotes were raised and sacrificed at days indicated for RNA extraction and cDNA synthesis. 4dpf group was normalized to 100% and all gene expression was normalized to the house-keeping gene, *ef1a or β–actin.* Results are expressed as mean + s.e.m.

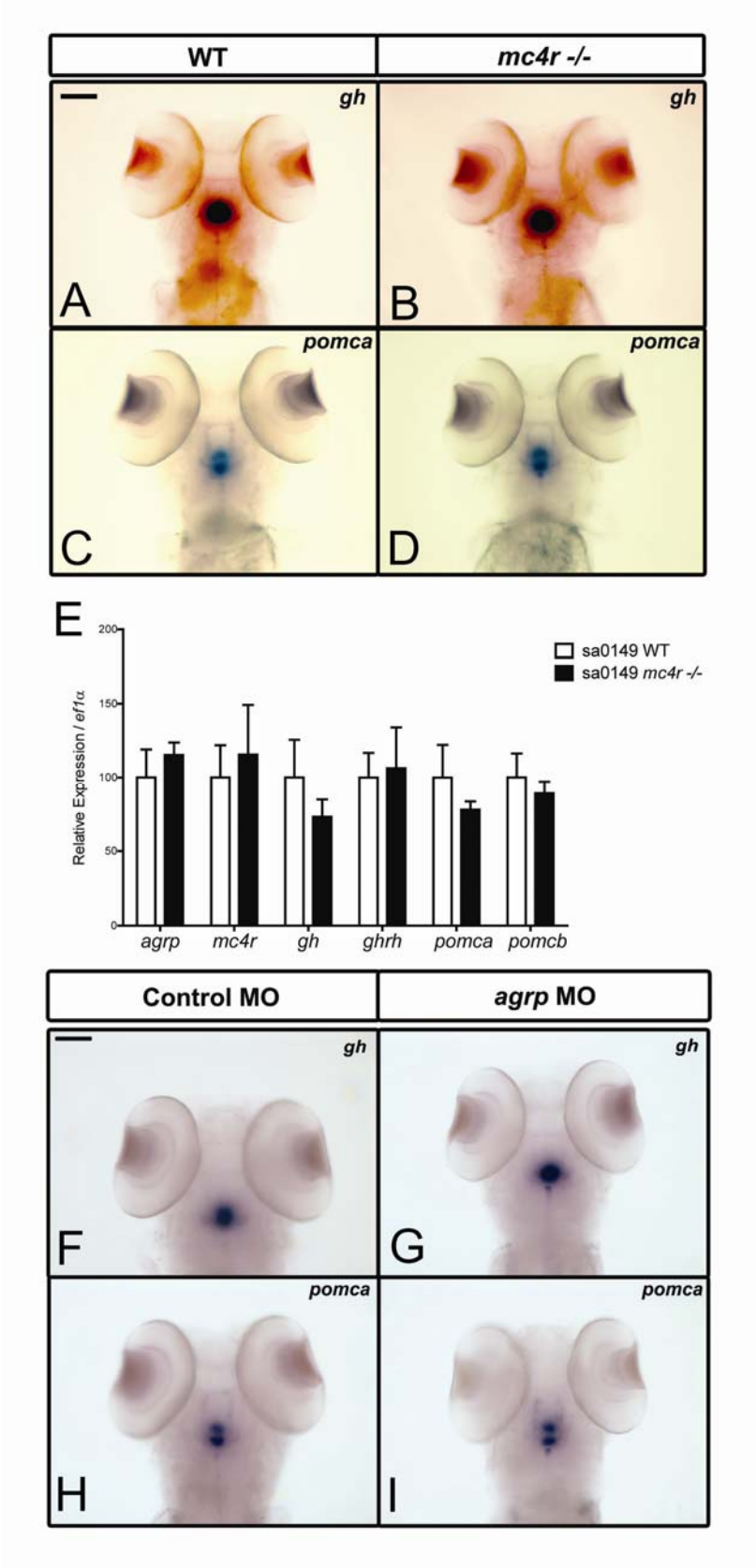

Figure S3. No Effect of *agrp* MO in the *mc4r-/-* Background

(A-D) Whole mount in situ hybridization of *gh* (A-B) and *pomca* (C-D) in uninjected sa0149 wild type fish (A and C) or un-injected sa0149 *mc4r* -/- fish (B and D) at 4dpf. Scale bar:

100µm. (E) Relative expression levels of *agrp, mc4r, gh, ghrh, pomca, pomcb* were analyzed by Q-PCR. Offspring from sa0149 sibling wild type and sa0149 *mc4r-/-* matings were raised at standard condition. 30 uninjected embryos from each condition were divided into 3 groups and sacrificed at 4dpf for RNA extraction and cDNA synthesis. Wild type group was normalized to 100% and all gene expression was normalized to the house-keeping gene, *ef1a.* Results are expressed as mean + s.e.m., and statistical analysis was done by unpaired t-test (Not Significant for all genes). (F-I) Whole mount in situ hybridization of *gh* (F-G) and *pomca* (H-I) in *mc4r* -/- fish injected with 2.5ng standard control (F and H) or *agrp* morpholino oligonucleotides (G and I). Scale bar: 100µm.

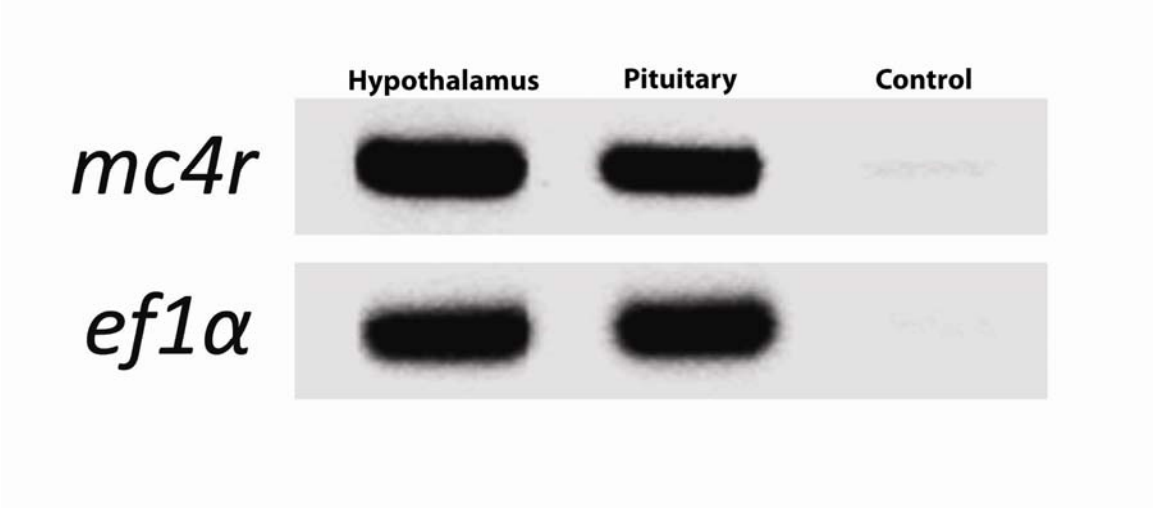

Figure S4. Expression of *mc4r* RNA in Zebrafish Pituitary.

RT-PCR amplification of *mc4r* and *ef1a* from zebrafish pituitary. Pituitary was carefully dissected and 1.9µg total RNA was extracted from 42 one year old WT adults. 10ng was used for each reaction as described in Experimental Procedures.